Orbital ordering in RVO_3 (R=Y,Tb) controlled by hydrostatic pressure

D. Bizen, K. Nakatsuka, T. Murata, H. Nakao, and Y. Murakami
Department of Physics, Tohoku University, Sendai 980-8578, Japan

S. Miyasaka
Department of Physics, Osaka University, Osaka 560-0043, Japan

Y. Tokura
Department of Applied Physics, University of Tokyo, Tokyo 113-8656, Japan
and Correlated Electron Research Center, National Institute of Advanced Industrial Science and Technology, Tsukuba 305-8562 Japan

(Received 15 July 2008; revised manuscript received 7 November 2008; published 15 December 2008)

Orbital ordered states of YVO_3 have been systematically investigated using the low-temperature and high-pressure x-ray diffraction technique. The pressure-temperature phase diagram for the orbital state is determined from the lattice constants and the reflection conditions. The phase diagram shows that the C-type orbital ordering (C-OO) is significantly stabilized relative to the G-type orbital ordering (G-OO) by application of hydrostatic pressure. Based on the result, we could achieve the $3d$-orbital state switching in $TbVO_3$ from the G-OO to the C-OO by applying pressure. The pressure effect on the orbital ordering is discussed from the viewpoint of the covalency among the R-ion d, the oxygen $2p$, and the vanadium $3d$ orbitals.

DOI: 10.1103/PhysRevB.78.224104 PACS number(s): 71.30.+h, 61.50.Ks, 61.05.cp

I. INTRODUCTION

Perovskite-type transition-metal oxides, RMO_3 (R: rare earth, M: transition metal), and the doped analogs show intriguing physical properties such as high T_C superconductivity,[1] colossal magnetoresistance effects,[2] magnetoelectric effects,[3] and so on. The strong coupling among charge, spin, orbital of the $3d$ electrons and lattice degrees of freedom causes these phenomena.[4] In particular the orbital ordering and related phenomena have attracted much attention.[5] In RMO_3, the energy level of $3d$ orbitals splits into the lower t_{2g} orbitals and the higher e_g orbitals owing to the crystal field in the MO_6 octahedron. In manganites the e_g orbital electron plays an important role in the physical properties while the t_{2g} orbital electron plays an important role in titanates and vanadates. These orbital ordered states have recently been clarified by the developed experimental techniques.[6–11]

In RVO_3 (R: rare earth or Y), the two valence electrons of V^{3+} ions occupy the near-triply degenerated t_{2g} orbitals. As a result, RVO_3 shows various physical properties coupled with the orbital and spin states. Two types of orbital ordering have been reported in RVO_3 systems.[12] One is C-type orbital ordering (C-OO) with the antiferroic arrangement of $d^1_{xy}d^1_{yz}$ and $d^1_{xy}d^1_{zx}$ in the ab plane and the ferroic arrangement along the c axis [Fig. 1(a)]. The other is G-type orbital ordering (G-OO) with the antiferroic arrangement in all the three orthogonal directions [Fig. 1(b)]. In RVO_3 (R=Tb-La) with a large R-ionic radius, the ground state is the G-OO state which is transformed to an orbitally disordered state at T_{OO1}. In YVO_3 with a relatively small R-ionic radius, on the other hand, the ground state is the C-OO state; the G-OO phase still survives in the intermediate temperature region ($T_{OO2} < T < T_{OO1}$).[13] The magnetic ordering of V^{3+} (S=1) in RVO_3 is dominated by the superexchange interaction, which strongly depends on the orbital state. The C-type spin ordering (C-SO) with the ferromagnetic coupling along the c axis and the antiferromagnetic coupling in the ab plane appears in the G-OO phase. The G-type spin ordering (G-SO) with antiferromagnetic coupling in all the three directions appears in the C-OO phase.[14–16]

The crystal structures in respective phases were investigated by x-ray and neutron diffractions.[14,17–19] The C-OO and the G-OO phases have an orthorhombic lattice with the space-group $Pbnm$ and a monoclinic one with $P2_1/b$, respectively. The orbital structures in the C-OO and the G-OO phases were determined by the anisotropy of VO_6 octahedron, i.e., Jahn-Teller distortion, obtained by the structure analysis. In the orbital disordered (OD) phase, on the other hand, the VO_6 octahedron is nearly isotropic although the space group is $Pbnm$. The lattice constants show anomalies at the respective transitions, T_{OO1} and T_{OO2}.[15,20,21] The change from the orthorhombic to the monoclinic lattice can be evaluated by the (4 0 1) reflection; the (4 0 1) reflection is a forbidden reflection in $Pbnm$ but a fundamental one in

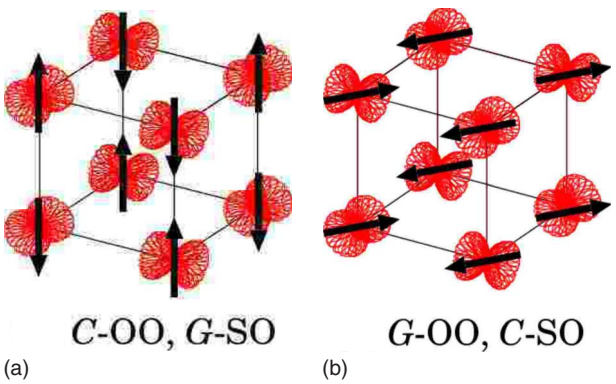

FIG. 1. (Color online) Schematic view of (a) the C-OO-G-SO and (b) the G-OO-C-SO. The orbital states are shown as the spatial electron-density distribution. The arrows represent the magnetic moment at each vanadium ions (Refs. 14 and 16).

$P2_1/b$. The intensity, which reflects the small atomic displacement due to the *G*-OO, is $\sim 10^{-4}$ times weaker than the strongest fundamental peak intensity. The deviation from 90° of the monoclinic angle α cannot be observed; the α seems to be very close to 90°.[14,17,18] Therefore, in this experiment the transition temperatures were determined by the measurements of the lattice constants and the intensity of (4 0 1) reflection and the monoclinic phase is identified by the reflection condition.

In the present work, we have studied the orbital states of YVO_3 and $TbVO_3$ under hydrostatic pressure. In these compounds the *G*-OO and *C*-OO states compete with each other: the ground states are located near the phase boundary between these orbital states. Thus, we can control the orbital states by applying hydrostatic pressure. The hydrostatic pressure has an advantage over the chemical one because the physical parameters can be controlled continuously without any sample problems, i.e., a randomness effect and a sample dependency; these will be the problems in the study of the chemical pressure effect by the substitution of ions. Recently, the studies of orbital state under the hydrostatic pressure were reported in the titanate and the manganite[22,23] where the change of the orbital state was observed. The pressure effect on the spin state in RVO_3 was also studied.[24] However, the ground state could not be changed by applying pressure since the pressure range under 1 GPa was rather low. In this paper, we describe the notable pressure effect as the one causing the change in the orbital ordering structure. The pressure-temperature phase diagram for the orbital state was studied in YVO_3 and $TbVO_3$ up to $\sim$10 GPa using the high-pressure low-temperature x-ray diffraction technique. We also tried to control the orbital state by applying the hydrostatic pressure.

II. EXPERIMENT

High-quality single crystals of RVO_3 (R=Y,Tb) were grown by a floating-zone method.[25] We cut and shaped the samples to be in a diamond-anvil cell (DAC); the typical size of samples was $\sim 100\times 100\times 30$ μm^3. For the high-pressure and low-temperature experiments, a helium gas-pressure driven DAC was mounted on a closed-cycle helium refrigerator. The culet sizes were 800, 600, and 500 μm. Either nitrogen or a 1:1 mixture of pentane and isopentane was used as a pressure-transmitting medium depending on the experimental pressure region. We carried out x-ray diffraction experiments, changing the sample temperature under a constant pressure. The sample pressure was controlled by the helium gas pressure so as to be kept constant while changing temperature. The pressure was calibrated from a lattice constant of NaCl enclosed with the sample in the DAC. The estimated pressure variation during the temperature change was less than 0.2 GPa. The single-crystal x-ray diffraction experiments with a four-circle diffractometer were performed using a rotating anode x-ray generator (XG) with a Mo target and synchrotron-radiation x-ray (SRX) beamlines BL-4C, BL-9C at Photon Factory, KEK. In the experiments using XG, the incident x-ray energy was monochromatized to 17.44 keV (Mo Kα) by a pyrolytic-graphite (0 0 2) monochromator. We used SRX in the experiments, requiring high angle resolution and high flux of incident x rays. The incident x ray was monochromatized at about 18 keV by double Si(1 1 1) crystals, and focused by a bent cylindrical mirror; the beam size was 0.6×0.7 mm^2.

III. RESULTS

A. YVO_3

The orbital ground state of RVO_3 transforms from *C*-OO into *G*-OO when the *R* ionic radius increases. With increasing radius, the V-O-V bond angle gradually approaches 180°.[14,17–19,26] In this case, the transfer integral t between the nearest-neighbor V ions, or equivalently the one-electron band width W, increases. Hence the ground state can be viewed as changing from *C*-OO to *G*-OO with increasing bandwidth. The bandwidth also increases by applying pressure as discussed in Sec. IV. Therefore, one might expect that the ground state of YVO_3 would change from *C*-OO to *G*-OO under high pressure. However, what we found in this study is the opposite tendency as described in the following. The pressure-induced volume contraction brings about a highly nontrivial consequence in the orbital orders.

The temperature dependence of the lattice constants a and b was measured at high pressure up to 7.5 GPa (Fig. 2). The lattice constants a and b were calculated from the peak positions of the (4 0 0) and the (0 2 0) reflections, respectively. The lattice constant b at 0.5 GPa shows a jump around 80 K, reminiscent of a first-order phase transition, and has a kink around 200 K [Fig. 2(b)]. The lattice constant a also shows a jump around 80 K at 0.7 GPa while no anomaly is observed at 200 K [Fig. 2(a)]. These results are consistent with those at ambient pressure reported previously.[15,20,21] Hence we assigned the phase transition around 200 and 80 K to the OD to *G*-OO transition at T_{OO1} and the *G*-OO to *C*-OO one at T_{OO2}, respectively. In this manner, the pressure dependence of T_{OO1} and T_{OO2} was determined as shown in Fig. 2. With increasing pressure, the T_{OO2} goes up. In contrast, T_{OO1} remains around 200 K up to 3 GPa. Above 3 GPa, the kink at T_{OO1} of the lattice constant b becomes obscure, and the transition temperature T_{OO1} could not be identified.

In order to examine the crystal symmetry above 3 GPa, we searched for the (4 0 1) reflection, which is forbidden in the symmetry *Pbnm* but allowed in $P2_1/b$. The (4 0 1) intensity was measured under high pressure as a function of temperature (Fig. 3). In the cooling process at 0.7 GPa, the (4 0 1) intensity gradually increases below T_{OO1} like a second-order phase transition and disappears abruptly at T_{OO2}. The temperature dependence is consistent with the previous report at ambient pressure.[17,18] Under higher pressure than 3 GPa, the (4 0 1) reflection was observed clearly and T_{OO1} could be unambiguously determined. Then, we find the decline of T_{OO1} above 3 GPa although $T_{OO1}(\sim 200$ K) does not change below 3 GPa. The (4 0 1) reflection is not detected at 7 GPa within the experimental accuracy, suggesting that the *G*-OO phase disappears above 7 GPa. However, the anomaly in the temperature dependence of the lattice constant b exists even at 7.5 GPa. Hence there may be a phase transition, which continuously connects with the transition at T_{OO2}.

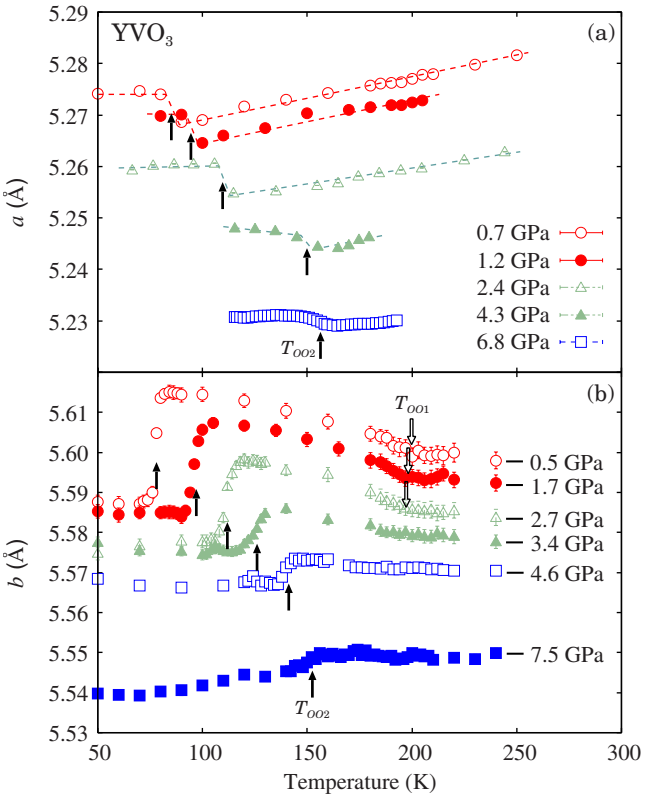

FIG. 2. (Color online) Temperature dependence of lattice constants (a) a and (b) b for YVO_3 up to 7.5 GPa. The lattice constants a and b were calculated from the peak positions of (4 0 0) and (0 2 0) reflections, respectively. The open and closed arrows indicate the transition temperature of the G-OO (T_{OO1}) and one of the C-OO (T_{OO2}), respectively. (a) The data were collected by using SRX. (b) The data were collected by using a rotating anode XG.

The pressure-temperature phase diagram of the orbital state for YVO_3 is summarized in Fig. 6. The G-OO/C-OO transition temperature T_{OO2} linearly goes up with increasing pressure $[dT_{OO2}/dP=18\pm1$ (K/GPa)]. The increase in T_{OO2} under pressure is consistent with the previous report.[24,27] By applying pressure, T_{OO2} reaches 160 K around 5 GPa; the transition temperature is the highest one in the studies of pressure effect and R-ion substitution.[13,24] Then, the G-OO phase disappears above 6 GPa. However, a phase transition still exists above 6 GPa, and the transition temperature corresponds to the OD/C-OO phase boundary (Fig. 6). The OD and C-OO phases have the same space-group $Pbnm$. Such a phase transition, which has not been reported up to now, will be argued later.

B. $TbVO_3$

The ionic radius of Tb^{3+} is larger than that of Y^{3+}; the orbital ground state of $TbVO_3$ is the G-OO at ambient pressure unlike the C-OO of YVO_3. In the previous section, we have shown that the C-OO is stabilized under pressure in YVO_3. Based on this observation, we tried to examine whether the ground state of $TbVO_3$ can be changed from G-OO to C-OO by applying pressure. The pressure-temperature phase diagram of $TbVO_3$ was determined by

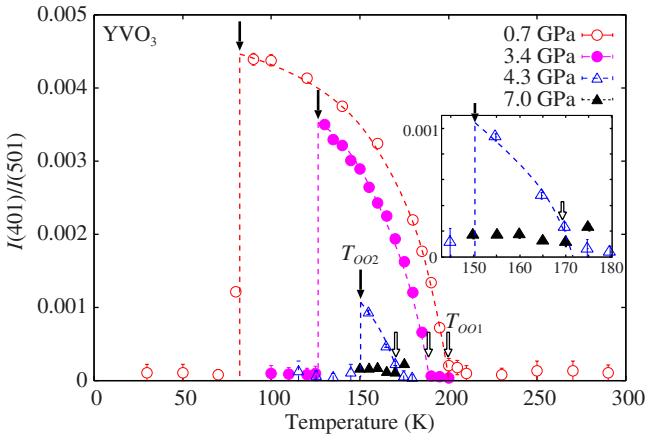

FIG. 3. (Color online) Temperature dependence of the (4 0 1) intensity for YVO_3 up to 7 GPa. The intensity of (4 0 1) forbidden reflection is normalized by that of (5 0 1) fundamental reflection. The open and closed arrows indicate T_{OO1} and T_{OO2}, respectively. The intensity in the C-OO and OD phase is the background level. The inset presents the magnified figure of the 4.3 and 7.0 GPa data. The data were collected by using SRX.

measurements of the lattice constant a and the (4 0 1) reflection. The temperature dependence of the lattice constant a was measured at 0.7 GPa (Fig. 4), which did not show such an anomaly. The intensity of the (4 0 1) reflection appears below $T_{OO1}=190$ K and survives even at 30 K (Fig. 5). Thus the orbital ground state remains as the G-OO phase at 0.7 GPa. On the other hand, the (4 0 1) intensity at 1.9 GPa suddenly disappears below 70 K. The disappearance of the (4 0 1) reflection suggests that the crystal symmetry becomes higher one than that of $P2_1/b$; namely the ground state is not the G-OO phase. The temperature dependence of lattice constant a shows a jump above 2 GPa (Fig. 4). The two-phase coexistence was also observed at the transition. These mean that the phase transition is of a first order. The observations resemble those of YVO_3 at ambient pressure. Therefore we assigned this structural phase transition to the G-OO to C-OO one at T_{OO2}.

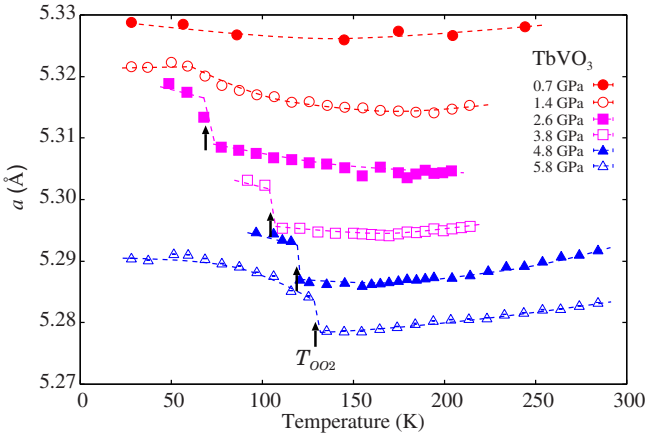

FIG. 4. (Color online) Temperature dependence of lattice constant a for $TbVO_3$ up to 5.8 GPa. The lattice constant a was calculated from the peak position of (4 0 0) reflection. The closed arrow indicates T_{OO2}. The data were collected by using SRX.

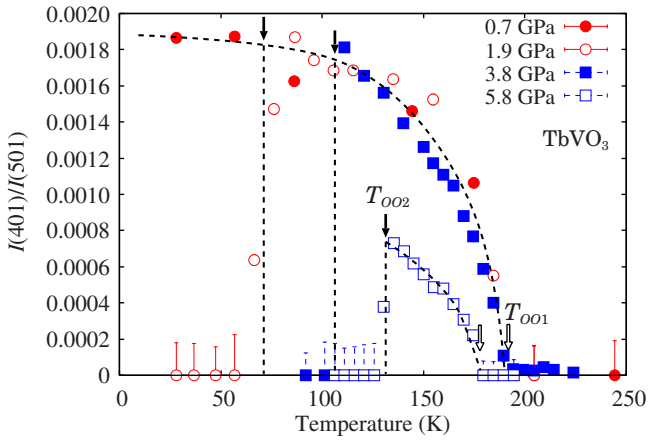

FIG. 5. (Color online) Temperature dependence of the (4 0 1) intensity for $TbVO_3$ up to 5.8 GPa. The intensity of (4 0 1) forbidden reflection is normalized by that of (5 0 1) fundamental reflection. The open and closed arrows indicate T_{OO1} and T_{OO2}, respectively. The data were collected by using SRX.

The pressure-temperature phase diagram of $TbVO_3$ is shown in Fig. 6. As expected, the ground state of $TbVO_3$ appears to change from *G*-OO to *C*-OO. The transition pressure is about 2 GPa. The transition temperature T_{OO1} does not change up to 5 GPa and decreases above this pressure. On the other hand, the transition temperature T_{OO2} linearly goes up with increasing pressure, and the slope $[dT_{OO2}/dP = 18 \pm 2$ (K/GPa)] is the same as that of YVO_3. The pressure dependence of T_{OO1} and T_{OO2} is quite similar to that in YVO_3. Hence the phase diagram of $TbVO_3$ can be well scaled with that of YVO_3 with the shift by 2 GPa. The phase diagram clearly indicates that the *C*-OO becomes more stable than the *G*-OO under applied pressures. We expect that the *G*-OO phase of $TbVO_3$ disappears above 8 GPa.

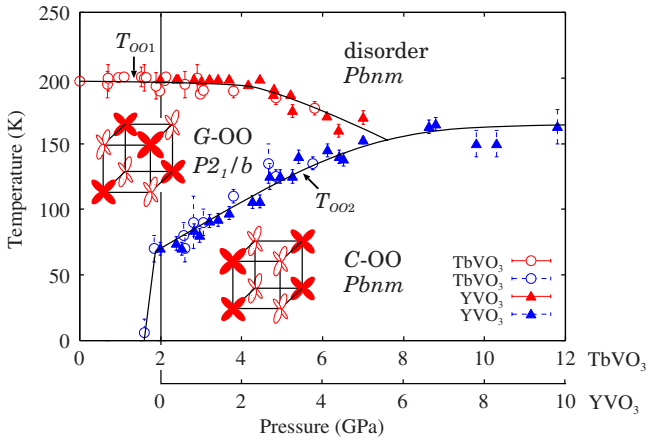

FIG. 6. (Color online) Pressure-temperature phase diagram of the orbital state for YVO_3 and $TbVO_3$ (Ref. 34). Open circles and closed triangles represent the phase-transition temperatures of $TbVO_3$ and YVO_3, respectively. The phase diagram of YVO_3 applies to be shifted as a whole to higher pressure by 2 GPa. Schematic of the *G*-OO and *C*-OO are also shown, in which lobes indicate occupied d_{yz} and d_{zx} orbitals on the vanadium ions. The d_{xy} orbital, which is displaced for clarity, occupies every vanadium site.

IV. DISCUSSION

The universal pressure-temperature phase diagram (Fig. 6) of the orbital states for RVO_3 was clarified in our low-temperature and high-pressure experiments. A marked result is that the ground state of RVO_3 changes from the *G*-OO to the *C*-OO with applying pressure: the *C*-OO phase is stabilized by the hydrostatic pressure as compared with the *G*-OO phase.

Here we discuss the mechanism stabilizing the *C*-OO phase under hydrostatic pressure. In the *R*-ion substitution studies, the ground state of the orbital ordering changes from the *C*-OO to the *G*-OO phase with increasing *R*-ion radius. There the bandwidth *W* is considered to be a key parameter since the *W* increases with increasing *R*-ion radius. Namely, the *G*-OO phase is stabilized by the increase in the *W*. In RMO_3, the *W* generally increases by applying pressure because of the contraction of the unit-cell volume and/or the increase in the *M*-O-*M* bond angle.[23,28] Loa *et al.*[23] studied the crystal structure and the band gap in $YTiO_3$, which has the analogous structure to RVO_3. There, the band gap decreases with applying pressure, indicating an increase in the *W*. The Ti-O-Ti bond angle changes only about $\pm 1°$ up to 16 GPa. Thus, they concluded that the enhancement of the *W* is caused by the contraction of the bond length. For RVO_3 system, consequently, we can expect that the *W* increases due to the contraction of the VO_6 octahedron and the *G*-OO phase stabilized by the applying pressure. However, this expectation is inconsistent with our result of the *C*-OO phase stabilization under high pressure.

To interpret the *C*-OO phase stabilization, we should take into account a covalency effect between V-3*d* and *R*-*d* orbitals, which is caused by the coupling via the O 2*p* orbital and the direct one. Several theories indicate that the covalency effect is important in determining the type of orbital ordering.[29–31] Under high pressure, the ions approach each other, owing to the contraction of the unit-cell volume, and the hybridization between these orbitals increases. Hence the covalency becomes one of important parameters in discussing the pressure effect for the orbital state. According to the crystal structure studies for YVO_3 at ambient pressure,[14,18] the distance between Y^{3+} and V^{3+} ions in the *C*-OO phase is closer than that in the *G*-OO phase. Therefore the covalent character is developed in the *C*-OO phase; the energy gain due to the covalency in the *C*-OO phase is larger than that in the *G*-OO phase. Hence it is likely that the *C*-OO is stabilized when the covalency effect increases under high pressure. We also note that the Y and Tb ions have different empty *d* orbitals, 4*d* and 5*d*, respectively, although the covalency effect between V-3*d* and *R*-*d* is simply discussed here. Arima and Tokura[32] studied the variation in the electric structures with the rare-earth element *R* in RMO_3. In their results La 5*d* and Y 4*d* have almost the same energy levels. Such a similarity in *R*-*d* orbital may explain that the universal phase diagram for RVO_3 was obtained.

Mizokawa and co-workers[29,30] theoretically estimated the energy deference among the orbital-spin ordering phases in RVO_3 by Hartree-Fock calculation, in which the bandwidth and covalency were considered as important parameters in determining the orbital ground state. In the calculation with-

out the covalency effect, the orbital ground state is independent of the bandwidth and always in the G-OO phase. On the other hand, the C-OO phase appears as the orbital ground state in the calculation with increasing covalency effect. They insisted that the covalency between the R-site cation d and the oxygen $2p$ orbitals stabilizes the C-OO phase. From these experimental and theoretical reasons, the stabilization of C-OO phase with increasing pressure can be understood not by the bandwidth effect but by the covalency effect.

Here we found the phase transition above 6 GPa in YVO_3, the transition temperature of which corresponds to the OD/C-OO phase boundary (Fig. 6). At this transition the space group does not change although the symmetry is usually broken at a phase transition. In LaMnO_3, the order-disorder phase transition of Mn e_g orbital without the change of the space group was actually reported.[33] Another possibility is the magnetic symmetry breaking upon the phase transition. The G-OO/C-OO transition at T_{OO2} accompanies the C-SO/G-SO magnetic transition. The G-OO/C-OO phase boundary appears to continuously connect with the OD/C-OO one with increasing pressure in the phase diagram (Fig. 6). Therefore, the magnetic ordering may occur at the OD/C-OO transition. To make clear the nature of the phase transition, the magnetic phase diagram under high pressure is also needed; we are carrying out neutron-diffraction experiments under high pressure and low temperature to determine the magnetic phase diagram.

Finally, we note the pressure effect on the G-OO phase. The OD/G-OO transition temperature, T_{OO1}, decreases with increasing pressure as shown in Fig. 6. Namely, the G-OO is suppressed by applying pressure. In general, a crystal lattice contracts and becomes hard under high pressure. Hence the energy gain due to the Jahn-Teller effect becomes small. The melting of orbital ordering under high pressure is actually observed in manganite systems.[22] We think that the decline of T_{OO1} is explained by this pressure effect.

V. CONCLUSION

We have investigated the pressure effects on the orbital states in $R\mathrm{VO}_3$. The pressure-temperature phase diagrams of the orbital state for $R\mathrm{VO}_3$(R=Y,Tb) were determined; the C-OO is stabilized as compared with the G-OO by applying hydrostatic pressure. Based on the result, we have succeeded in controlling the ground state of TbVO_3 from the G-OO to the C-OO by applying pressure. We presented the global pressure-temperature phase diagram for the orbital state of $R\mathrm{VO}_3$ (R=Y,Tb) and proposed that the covalency stabilized the C-OO phase under high pressure.

ACKNOWLEDGMENTS

We thank T. Arima and S. Ishihara for fruitful discussions. Technical support by Y. Wakabayashi and H. Sawa is also appreciated. The study using synchrotron x-ray has been performed under the approval of the Photon Factory Program Advisory Committee (Proposals No. 2005G134 and No. 2007G582).

[1] For a review, *Physical Properties of High Temperature Superconductors*, edited by D. M. Ginzburg (World Scientific, Singapore, 1992).
[2] For a review, *Colossal Magnetoresistive Oxides*, edited by Y. Tokura (Gorden and Breach Science, New York, 2000).
[3] T. Kimura, T. Goto, H. Shintani, K. Ishizaka, T. Arima, and Y. Tokura, Nature (London) **426**, 55 (2003).
[4] M. Imada, A. Fujimori, and Y. Tokura, Rev. Mod. Phys. **70**, 1039 (1998).
[5] Y. Tokura and N. Nagaosa, Science **288**, 462 (2000).
[6] Y. Murakami, H. Kawada, H. Kawata, M. Tanaka, T. Arima, Y. Moritomo, and Y. Tokura, Phys. Rev. Lett. **80**, 1932 (1998).
[7] Y. Murakami *et al.*, Phys. Rev. Lett. **81**, 582 (1998).
[8] F. Iga *et al.*, Phys. Rev. Lett. **93**, 257207 (2004).
[9] S. B. Wilkins, P. D. Spencer, P. D. Hatton, S. P. Collins, M. D. Roper, D. Prabhakaran, and A. T. Boothroyd, Phys. Rev. Lett. **91**, 167205 (2003).
[10] A. Koizumi, S. Miyaki, Y. Kakutani, H. Koizumi, N. Hiraoka, K. Makoshi, N. Sakai, K. Hirota, and Y. Murakami, Phys. Rev. Lett. **86**, 5589 (2001).
[11] M. Ito, N. Tuji, F. Itoh, H. Adachi, E. Arakawa, K. Namikawa, H. Nakao, Y. Murakami, Y. Taguchi, and Y. Tokura, J. Phys. Chem. Solids **65**, 1993 (2004).
[12] M. Noguchi, A. Nakazawa, S. Oka, T. Arima, Y. Wakabayashi, H. Nakao, and Y. Murakami, Phys. Rev. B **62**, R9271 (2000).
[13] S. Miyasaka, Y. Okimoto, M. Iwama, and Y. Tokura, Phys. Rev. B **68**, 100406(R) (2003).
[14] M. Reehuis, C. Ulrich, P. Pattison, B. Ouladdiaf, M. C. Rheinstädter, M. Ohl, L. P. Regnault, M. Miyasaka, Y. Tokura, and B. Keimer, Phys. Rev. B **73**, 094440 (2006).
[15] H. Kawano, H. Yoshizawa, and Y. Ueda, J. Phys. Soc. Jpn. **63**, 2857 (1994).
[16] C. Ulrich, G. Khaliullin, J. Sirker, M. Reehuis, M. Ohl, S. Miyasaka, Y. Tokura, and B. Keimer, Phys. Rev. Lett. **91**, 257202 (2003).
[17] G. R. Blake, T. T. M. Palstra, Y. Ren, A. A. Nugroho, and A. A. Menovsky, Phys. Rev. Lett. **87**, 245501 (2001).
[18] G. R. Blake, T. T. M. Palstra, Y. Ren, A. A. Nugroho, and A. A. Menovsky, Phys. Rev. B **65**, 174112 (2002).
[19] P. Bordet, C. Chaillout, M. Marezio, Q. Huang, A. Santoro, S.-W. Cheong, H. Takagi, C. S. Oglesby, and B. Batlog, J. Solid State Chem. **106**, 253 (1993).
[20] M. H. Sage, G. R. Blake, C. Marquina, and T. T. M. Palstra, Phys. Rev. B **76**, 195102 (2007).
[21] M. Sikora, C. Marquina, M. R. Ibarra, A. A. Nugroho, and T. T. M. Palstra, J. Magn. Magn. Mater. **316**, e692 (2007).
[22] I. Loa, P. Adler, A. Grzechnik, K. Syassen, U. Schwarz, M. Hanfland, G. K. Rozenberg, P. Gorodetsky, and M. P. Pasternak, Phys. Rev. Lett. **87**, 125501 (2001).
[23] I. Loa, X. Wang, K. Syassen, H. Roth, T. Lorenze, M. Hanfland, and Y.-L. Mathis, J. Phys.: Condens. Matter **19**, 406223 (2007).
[24] J.-S. Zhou, J. B. Goodenough, J.-Q. Yan, and Y. Ren, Phys. Rev.

Lett. **99**, 156401 (2007).
[25] S. Miyasaka, J. Fujioka, M. Iwama, Y. Okimoto, and Y. Tokura, Phys. Rev. B **73**, 224436 (2006).
[26] M. J. Martínez-Lope, J. A. Alonso, M. Retuerto, and M. T. Fernández-Díaz, Inorg. Chem. **47**, 2634 (2008).
[27] D. Bizen, K. Nakatsuka, H. Nakao, Y. Murakami, S. Miyasaka, and Y. Tokura, J. Magn. Magn. Mater. **310**, 785 (2007).
[28] J. Zhao, N. L. Ross, and R. J. Angel, Acta Crystallogr., Sect. B: Struct. Sci. **B60**, 263 (2004).
[29] T. Mizokawa, D. I. Khomskii, and G. A. Sawatzky, Phys. Rev. B **60**, 7309 (1999).
[30] T. Mizokawa and A. Fujimori, Phys. Rev. B **54**, 5368 (1996).
[31] M. De Raychaudhury, E. Pavarini, and O. K. Andersen, Phys. Rev. Lett. **99**, 126402 (2007).
[32] T. Arima and Y. Tokura, J. Phys. Soc. Jpn. **64**, 2488 (1995).
[33] J. Rodríguez-Carvajal, M. Hennion, F. Moussa, A. H. Moudden, L. Pinsard, and A. Revcolevschi, Phys. Rev. B **57**, 3189(R) (1998).
[34] The phase transition at T_{OO2} is of the first order, and T_{OO2} depends on the measurement process, cooling or warming. However, the hysteretic difference of T_{OO2} is less than 5 K, which is smaller than this experimental error of T_{OO2}. Therefore, the measuring process does not affect the phase diagram, although T_{OO2}'s determined by the warming and cooling processes are plotted simultaneously in the phase diagram.